https://doi.org/10.5194/egusphere-2024-2787
Preprint. Discussion started: 7 October 2024

Vapor pressure deficit plays a pivotal role in the carbon dioxide sink of the Jingxin Wetland

Jihao Zhang[1], Pengshen Chen[1], Duqi Liu[1], Ruihan Liang[1], Guishan Cui[1,2]

[1]College of Geography and Ocean Sciences, Yanbian University, Yanji, 133002, China
[2]Tumen River Basin Wetland Ecosystem Field Scientific Research and Observation Station, Yanji, 133002, China

Correspondence to: Guishan Cui (cuiguishan@ybu.edu.cn)

Abstract. Large uncertainties exist in the carbon sink and energy balance of wetland ecosystems under climate change conditions. This can be attributed, in part, to the limited understanding of the simultaneous impact of climate and carbon dynamics as well as that of energy equilibria. In addition, the temporal patterns and interconnections of carbon dynamics and energy equilibria, as inferred from ground observations, remain ambiguous. In this study, carbon dioxide flux data of the Jingxin Wetland from August 2021 to August 2023 were analyzed to evaluate the relative influence of climate change on the net ecosystem exchange (NEE) and energy equilibrium. The findings demonstrate that the Jingxin Wetland has a formidable capacity for carbon sequestration. Furthermore, the vapor pressure deficit (VPD) emerged as a key determinant of ecosystem carbon flux, whereas latent heat flux (LE) serves as the primary consumer of net radiation. Throughout the research period, net radiation (Rn) accounted for 73.5% of the total radiation. During both vegetation growth and dormancy seasons, Rn emerged as a principal factor influencing LE, which in turn affected the state of carbon cycling in the wetland ecosystems by impacting variations in the VPD during the growing season. Overall, our research outcomes shed light on the interplay between climate, carbon cycles, and energy budgets in wetland ecosystems, offering valuable insights for future investigations and conservation endeavors.

1 Introduction

Wetlands have gained considerable attention as focal points in carbon cycle research because of their substantial capacity for carbon storage (Wei and Wang, 2017). Numerous studies have documented the impacts of climate change on ecosystems, with an emphasis on the heightened sensitivity of ecosystems in high-latitude regions to climatic variations (Schuur et al., 2008); however, there is currently no consensus within the academic community on whether wetlands function as carbon sources or sinks in the carbon cycle (Du et al., 2021). While the vast majority of studies suggest that wetland ecosystems act as carbon sinks, meaning that they can absorb and store significant amounts of carbon and, thereby, mitigate climate change, ongoing global climate and environmental changes have led some wetlands acting as carbon sources. This underscores the complexity of the impacts of climate change on the carbon-storage capacity of wetlands (Wei and Wang, 2017). Changes in wetland climate not only affect the gross primary productivity (GPP) of wetland ecosystems but also ecosystem respiration

https://doi.org/10.5194/egusphere-2024-2787
Preprint. Discussion started: 7 October 2024

(Reco), and there are many uncertainties surrounding these two processes, making it challenging to quantify the difference between the two in terms of wetland net ecosystem exchange (NEE). Energy balance is a fundamental driver of climate formation and change, and climate change is realized through changes in near-surface energy, which influence regional climate change and, thus, ecosystem-level carbon cycles (Helbig et al., 2017). Broadly speaking, latent and sensible heat serve as bridges connecting meteorological changes to the carbon cycle; they interact with climatic factors and collectively influence the functionality of the Earth's climate system and ecosystems. Thus, by understanding these processes and their interrelationships, we can better predict the impact of climate change on ecosystems and regulate the Earth's energy and carbon balance by managing vegetation cover and water resources. In recent years, an increasing amount of research has focused on energy and carbon dioxide exchanges in different types of wetlands. Observations indicate that most wetlands in the Arctic and northern regions act as carbon sinks, with an annual carbon dioxide uptake of less than 100 g C m-2 yr-1 (Coffer and Hestir, 2019). In temperate regions, intact wetlands can absorb up to 250 g C m-2 yr-1 of carbon dioxide (Fang et al., 2018); however, among the various types of wetlands, cold-region wetlands are particularly sensitive to climate change. Specifically, cold-region wetlands, which are characterized by low temperatures and the presence of permafrost or seasonal frost, are a relatively unique type of wetland as they possess a significantly higher carbon-storage capacity than other types of wetlands and play an extremely important role in the entire terrestrial carbon cycle (Wei et al., 2020).

China has one of the richest wetland resources in the world, where wetlands in cold zones account for more than 60% of the natural wetlands. Owing to their distinctive structural and functional attributes, wetlands in cold zones show heightened susceptibility to shifts in climate and environmental conditions compared to other wetland ecosystems (Tan et al., 2011). For example, wetlands in cold regions are characterized by low temperatures and the presence of perennial or seasonally permanent frozen soil layers and, compared to other types of wetlands, they exhibit a higher level of carbon storage (Wang et al., 2016). Prior research has examined CO2 and heat fluxes in diverse types of cold wetlands. For example, Helbig and Chasmer (Helbig et al., 2017) employed static box gas chromatography to establish that the alpine marsh wetland of Swan Lake in Bayinbuluk, situated in the heart of the Tianshan Mountains, served as a carbon source. Shen et al. also discovered that a marshy wetland located in the cold region of the northeast corner of the Qinghai-Tibet Plateau functioned as a carbon source. Conversely (Shen et al., 2019), Wang et al. utilized the eddy covariance technique for long-term observations and discovered that high-altitude marsh wetlands in the Qinghai-Tibet region act as a significant carbon sink; and Zhu et al. used the eddy covariance method to investigate the carbon sink capacity of the Luanhaizi Wetland in Qinghai. (Wang et al., 2016; Zhu et al., 2020)

Under the trend of global warming, cold wetland drying and warming can also affect the thermal balance of wetland surfaces, leading to changes in the carbon-storage capacity of wetland ecosystems (Liu et al., 2019; Tan et al., 2011). For example, researchers have discovered that temperate forested wetlands in the Little Xingan Mountains act as carbon sinks; however, the carbon-sequestration capacity of these wetlands has been altered due to climate warming and permafrost degradation (Han et al., 2023; Wang et al., 2022). In addition, in the context of global climate change, carbon exchange is affected by a variety of environmental factors, such as air and soil temperatures, photosynthetically active radiation, precipitation, and

https://doi.org/10.5194/egusphere-2024-2787
Preprint. Discussion started: 7 October 2024

mean water depth, and the effects of environmental factors on CO2 fluxes are usually nonlinear (Chapin et al., 2002; Hao et al., 2011b; Zhu et al., 2020). However, the number of long-term flux observation stations in the cold wetlands of China is limited, and while the carbon fluxes and influencing factors of various wetland types in the Tibetan Plateau have been examined, there is a lack of research on carbon fluxes in cold wetlands in northeastern China. Notably, the scarcity of data from ground-based stations hinders the provision of reliable and comprehensive data needed to simulate the regional-scale carbon budget and balance (Fawei et al., 2008b; Liu et al., 2009).

Accurate and long-term measurements of carbon and energy fluxes are integral to enhancing our understanding of the relationships between wetland ecosystems and the atmosphere. A precise understanding of these fluxes and their environmental mechanisms can facilitate reasonable estimations of wetland carbon balances at an appropriate spatial scale. Advancements in eddy covariance techniques have enabled the direct measurement of CO2 and heat fluxes between terrestrial ecosystems and the atmosphere. In recent years, this approach has proved a primary method for determining the exchange fluxes of carbon dioxide between the atmosphere and ecosystems as well as land–air energy fluxes (Neubauer and Verhoeven, 2019). Indeed, eddy covariance techniques are widely recognized by meteorologists and ecologists for their ability to measure the exchange of carbon and heat fluxes in the atmosphere and at the Earth's surface. NEE observed using this meteorological method provides crucial insights into photosynthesis and respiration at the ecosystem scale. In addition, wetland plant phenology can provide key parameters for predicting wetland carbon balance (Liu et al., 2019). Therefore, wetland phenology studies can provide a temporal characterization of vegetation growth that is closely linked to CO2 exchange in wetlands.

The role of the Jingxin Wetland in China as a carbon source or sink is not yet definitively understood. This study, leverages observed data on carbon dioxide fluxes in the Jingxin Wetland from August 2021 to August 2023 to explore the characteristics and disparities in daily carbon flux mechanisms during the growing and non-growing seasons. Furthermore, the impact of carbon dioxide fluxes on climate is examined, focusing on the extent of the influence of diverse environmental factors and the state of the thermal equilibrium across different time scales. The specific aims of this study are to (a) unravel the characteristics of variations in NEE and carbon-sequestration capacity at diverse temporal scales in the Jingxin Wetland; (b) examine the correlations between climatic factors and carbon dioxide fluxes at multiple temporal scales, and determine their impact on NEE; and (c) further explain the impact of heat distribution on microclimates to illustrate the interconnections between heat, meteorological conditions, and CO2 flux.

2 Materials and methods

2.1 Site description

The Jingxin Wetland is situated on the Jingxin Plain, south of Hunchun City, within the Yanbian Korean Autonomous Prefecture, Jilin Province, China. It lies at the tripoint of China, North Korea, and Russia, and forms part of the lower Tumen River Basin. The geographic coordinates range from 42°27' N to 42°40' N and from 130°25' E to 130°39' E, with an

https://doi.org/10.5194/egusphere-2024-2787
Preprint. Discussion started: 7 October 2024

elevation of between 5 and 15 m above sea level (Fig. 1). The Jingxin Wetland, situated adjacent to the Sea of Japan, experiences a mesothermal oceanic monsoon climate characterized by pronounced oceanic influences. The region has well-defined wet and dry seasons, with 90% of the annual precipitation occurring during the growing season, which extends from April to October. The annual rainfall ranges from 800 to 950 mm; and the average annual temperature is 5.6 °C, with recorded extremes of +36.3 °C and −32.5 °C. Geographical proximity to the Sea of Japan, combined with the influence of the southeasterly sea breeze, results in distinct climatic features compared to regions at the same latitude, such as mild winters, cool summers, robust monsoons in spring and autumn, frequent cloud cover, diminished light levels, and elevated precipitation (Liu et al., 2009; Rankin et al., 2018). The area has a frost-free period of 156 d.

The Jingxin Wetland has rich biodiversity and high productivity, supporting 305 species of higher plants from 51 families. These species account for 14.59% of the total higher plant species in the Tumen River Basin and 60.76% of those in the wetlands within the province, thereby highlighting the wetland's botanical diversity (Sun et al., 2017). Primarily, vegetation such as reeds and wula sedges is distributed within the area covered by the carbon flux tower equipment. In contrast to the cold wetlands in China's Qinghai-Tibet region, the Jingxin Wetland is characterized by its low elevation, high average temperature, shorter land-freezing duration, and comparatively high vegetation productivity.

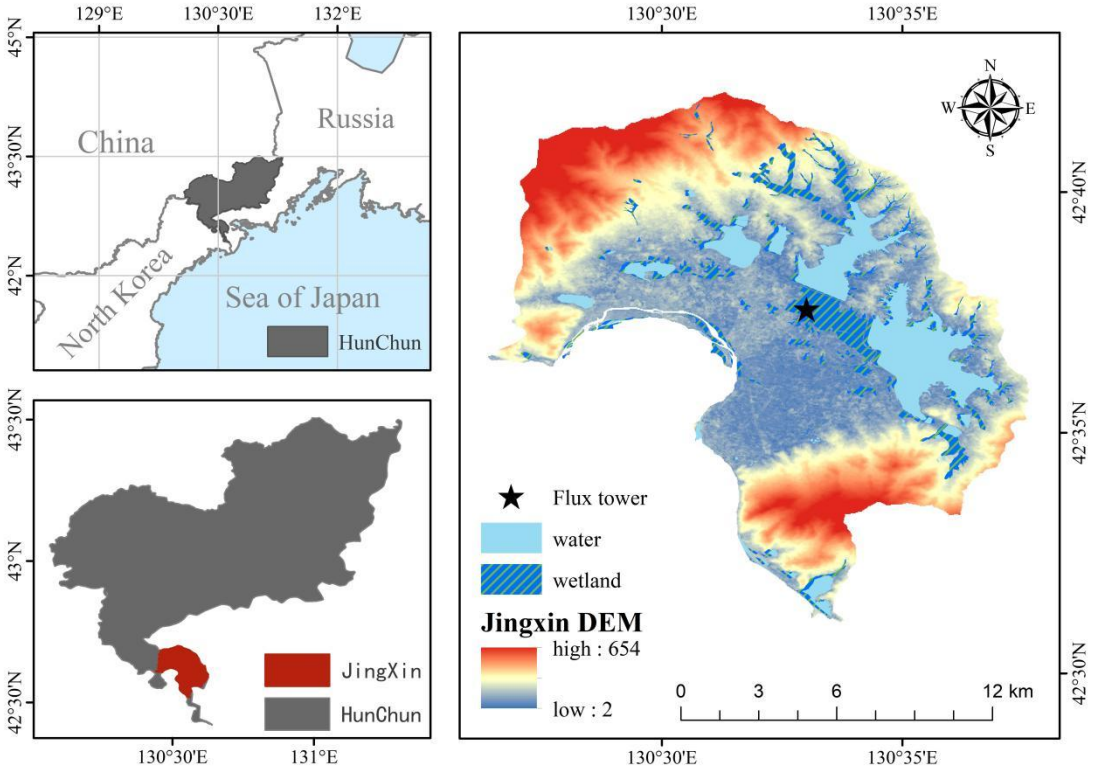

Figure 1: Jingxin Wetland flux tower (star) observation site location and elevation.

https://doi.org/10.5194/egusphere-2024-2787
Preprint. Discussion started: 7 October 2024

2.2 Data sources

An open-path eddy covariance flux observation system was used to continuously observe the net CO2 exchange between the Jingxin Wetland ecosystem and atmosphere in the Wudaopao area in the lower reaches of the Tumen River. The eddy covariance tower was composed of an open-path CO2/H2O analyzer (LI-7500, LICOR, Lincoln, USA), a three-dimensional ultrasonic anemometer (CSAT3, Campbell Scientific, Logan, USA), and a data logger (CR3000, Campbell Scientific, Logan, USA). An environmental element observation system was concurrently employed to monitor the following environmental variables: temperature (Ta, °C), vapor pressure deficit (VPD, hPa), photosynthetic photon flux density (PPFD, umol m-2 s-1), and precipitation (PPT, mm). Furthermore, heat flux data, including net radiant energy (Rn, W m-²), latent heat energy (LE, W m-²), and sensible heat energy (H, W m-²), were documented. The data collector recorded raw data at a frequency of 10 Hz. The mean values of the normalized vegetation index (NDVI) for three years (2020–2022) were extracted using the MODIS vegetation index product for the wetlands in Jingxin Township (MOD13, spatial resolution = 250 m, temporal resolution = 16 d; https://data.tpdc.ac.cn) to calculate the length of the growing season.

2.3 Preprocessing

The NDVI of the Jingxin Wetland was extracted using MATLAB for a period of three years. The software was also employed to calculate the start of the growing season (SOS) and end of the growing season (EOS) using the dynamic threshold method. These data were then integrated with information from a phenology camera (Trail camera, 24MP/1080P@30FPS) to accurately determine the SOS and EOS dates of the Jingxin Wetland.

NEE was calculated using EddyPro software with wild-point removal, coordinate rotation, Webb, Pearman, and Leuning (WPL) correction, and a storage term for 10 Hz raw flux observations (Vickers and Mahrt, 1997; Webb et al., 1980; Wilczak et al., 2001). The corrected energy balance comprising heat flux (H), latent heat flux (LE), and net radiation (Rn), and NEE and the environmental factors during the corresponding time period were obtained by removing the data during the same period of precipitation and excluding unreasonable fluxes smaller than a threshold value (± 3.5 standard deviations) using friction velocity (u*). Data quality control and culling led to missing data; therefore, to obtain a more continuous carbon dioxide flux record, data gaps with a real-time length of < 3 h were filled using linear interpolation (Zhao et al., 2010). For extended periods of missing data, the Marginal Distribution Sampling (MDS) method—a feature of the Tovi flux data-processing software (version 2.9.1)—was employed for flux data interpolation. This method is particularly effective for interpolating NEE data across larger spans of missing time, and has been used extensively in the field.

To denote carbon uptake by vegetation, the NEE of an ecosystem is typically negative. If only biological fluxes are considered, while the net ecosystem productivity (NEP) is numerically equivalent to NEE, albeit with an inverse sign (Zhao et al., 2022). NEE is the difference between GPP and Reco and is expressed by Equation (1). GPP refers to the rate at which ecosystem plants convert solar energy into organic matter through photosynthesis. This conversion is typically quantified as an increase in biomass per unit area or time, signifying the total energy produced by plants within a given ecosystem. Reco

https://doi.org/10.5194/egusphere-2024-2787
Preprint. Discussion started: 7 October 2024

denotes the net accumulation of carbon in an ecosystem, considering autotrophic respiration, heterotrophic respiration, and other forms of carbon consumption. Currently, the primary approaches to NEE partitioning involve the use of nighttime and daytime NEE data. Here, we used the nighttime partition method with the assumption that vegetation respiration is solely related to temperature (Ta) and that only respiration occurs at night. This can be modeled using the respiration equations of Lloyd and Taylor (Lloyd and Taylor, 1994), which extrapolate ecosystem respiration as a function of temperature to daytime ecosystem respiration fluctuations, as expressed in Equation (2):

$$NEE = \mathrm{Reco} - GPP \tag{1}$$

$$\mathrm{Reco} = rb * \exp\left(E_0 \left(\frac{1}{T_{ref} - T_0} - \frac{1}{T_{air} - T_0} \right) \right) \tag{2}$$

where rb (mol C m-2 s-1) is the basal respiration at the reference temperature; Tref (°C) is set to 15 °C; Eo (°C) is temperature sensitivity; Tair is air temperature; and the parameter T0 is the constant –46.02 °C. Daytime NEE was interpolated by fitting the relationship between nighttime NEE and air temperature, and GPP was obtained using Equation (1).

Flux data for NEE, GPP, and Reco were examined at daily, monthly, seasonal, and annual intervals. We analyzed the spatial and temporal variations in environmental factors and CO2 fluxes (NEE, GPP, and Reco) across different ecosystems over a 24-month period (August 2021 to August 2023). Environmental data corresponding to this period were also included in the analysis.

2.4 Analysis

We employed Pearson's correlation analysis to determine the relationship between wetland CO2 exchange and a range of climatic factors on a half-hour basis. Additionally, we examined the correlations between the energy budget and climatic factors. The effects of environmental factors on CO2 fluxes and environmental factors were examined on a whole-day scale using partial least squares regression (PLS). To investigate the influence of climatic factors on wetland CO2 fluxes during the growing and non-growing seasons, the influence of each environmental factor was calculated using multiple linear regression. The interaction between energy balance and meteorological factors was explored using multiple linear regression to understand the control and impact of the heat balance on the climate factors in wetland ecosystems. The coupling relationship between heat balance and carbon dioxide flux was also explained based on the role of the heat balance.

https://doi.org/10.5194/egusphere-2024-2787
Preprint. Discussion started: 7 October 2024

3 Results and discussion

3.1 Phenology in the Jingxin Wetland

This study used flux data from different phenological periods, analyzed images captured using a phenological cameras near the flux tower, and wetland NDVI data to depict the growing and non-growing seasons (Fig. 2(a), (b)). Subsequently, the temporal variations in net ecosystem carbon dioxide exchange during these periods was investigated. The results indicate that the start of SOS for wetland vegetation in Jingxin Town, located in the lower reaches of the Tumen River, consistently occurred approximately on the 110th day, on approximately April 14th, over the past three years. Conversely, the EOS typically began approximately on the 275th day, on approximately October 1st (Fig. 2(c)). During the SOS period, the vegetation transitioned from spring germination to vigorous growth, heralding the onset of increased total primary productivity within the wetland ecosystem; ecological activity in the wetland became more pronounced, with plants initiating photosynthesis. Conversely, during the EOS, the vegetation gradually entered a withering phase, signifying a slowdown in growth; vegetation life processes began to wane until complete withering occurred, accompanied by a decline in both photosynthesis and respiration. The surrounding vegetation community near the Jingxin Wetland Flux Tower began to exhibit signs of regression between 110 and 150 d, similar to the average SOS observed for marshy wetlands in the northeast (Shen et al., 2019).

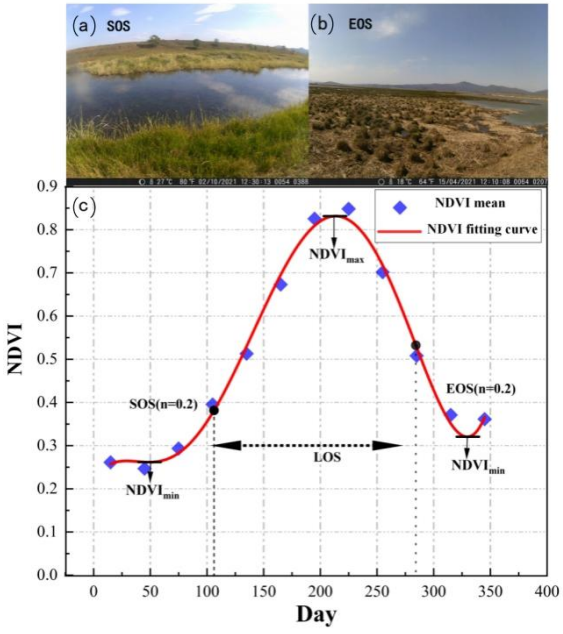

Figure 2: Duration of the wetland phenological period. (a). Phenological pictures of the beginning of the growing season of the Jingxin Wetland Ecosystem. (b). Phenological pictures of the end of the growing season of the Jingxin Wetland Ecosystem. (c). Phenology of the Jingxin Wetland was calculated using fitted curves of the Normalized Difference Vegetation Index (NDVI).

https://doi.org/10.5194/egusphere-2024-2787
Preprint. Discussion started: 7 October 2024

3.2 Meteorological conditions in the Jingxin Wetland

Daily and seasonal variations in the main meteorological variables from August 2021 to August 2023 are shown in Fig. 3. The daily average VPD exhibited significant seasonal variations during the study period, as shown in Fig. 3(a), with greater fluctuations during the growing season and smaller fluctuations during the non-growing season. Throughout the study period, the VPD ranged from 0 to 14.19 hPa, with amaximum of 14.19 hPa occurring on August 22, 2022. The daily maximum average PPFD occurred on June 7, 2022, reaching 697.3 umol m-2 s-1, while the daily minimum average PPFD occurred on November 30, reaching 11.50 umol m-2 s-1. Between June and July, there was a significant overall difference in the daily average PPFD; however, during the non-growing season, the daily average PPFD exhibited noticeably smaller fluctuations (Fig. 3(b)). Precipitation was predominantly concentrated during the growing season (June, July, and August), accounting for approximately 89% of the total precipitation during the study period. This coincided with a period of vigorous vegetation growth and the high temperatures typical of summer (Fig. 3(c)). The daily average temperature (Ta) also exhibited pronounced seasonal variations, reaching its peak in early August and its lowest in late January (Fig. 3(d)). The daily average temperature ranged from –20.8 ℃ to 29.8 ℃. The average wind speed exhibited a gradual change during the growing season, whereas it showed larger fluctuations during the non-growing season, with a maximum of 11.21 m s-1 (Fig. 3(e)).

https://doi.org/10.5194/egusphere-2024-2787
Preprint. Discussion started: 7 October 2024

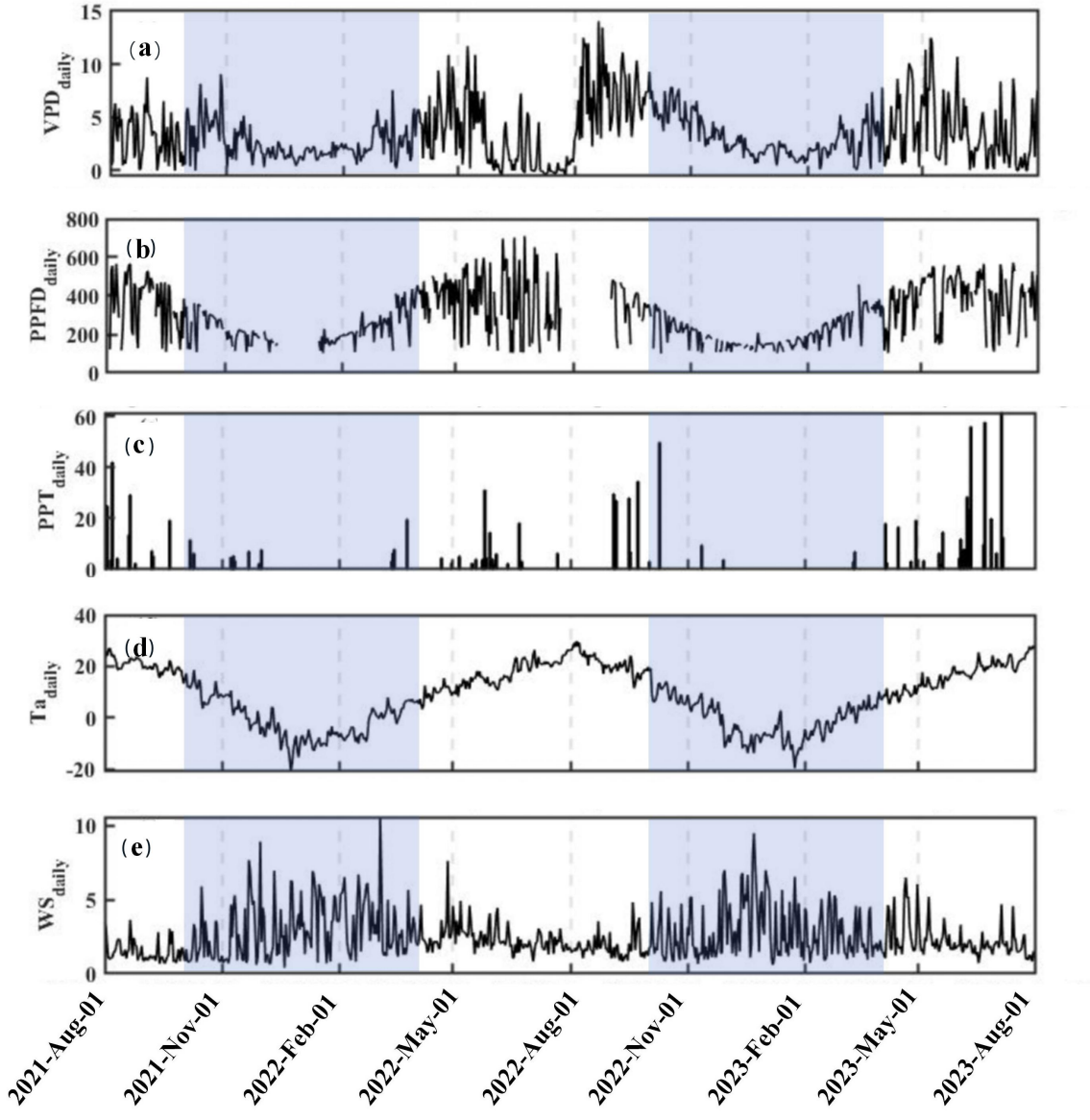

Figure 3: Diurnal variations in climatic variables between August 2021 and July 2023. (a). Daily average vapor pressure deficit (VPD, hPa). (b). Daily average photosynthetic photon flux density (PPFD, umol m-2s-1). (c). Daily sum of precipitation (PPT, mm d-1). (d). Daily average air temperature (Ta, ℃). (e). Daily average wind speed (WS, m s-1).

https://doi.org/10.5194/egusphere-2024-2787
Preprint. Discussion started: 7 October 2024

3.3 Variation and drivers of CO2 fluxes in the Jingxin Wetland

3.3.1 Daily variations of CO2 flux

The absorption of carbon dioxide in the Jingxin Wetland showed clear daily change characteristics across all months (Figs. 4 and S1). Throughout the months of growth (April to October), following day-break (04:30 to 06:30), the absorption of carbon dioxide through photosynthesis gradually surpassed the emissions from respiration. NEE became negative, transforming the ecosystem into a carbon sink, reaching its peak at 11:00–11:45. The zenith of the monthly average daily CO2 absorption was observed in June 2023, at 16.91 umol m-2 s-1. Conversely, during the same growing period, monthly CO2 emissions peaked during the night-time hours (0:00–2:00), with the highest rate occurring in August 2021, at 5.81 umol m-2 s-1. The daily variation in CO2 flux in the wetland showed a "U-shaped curve," which is consistent with the results of previous studies on wetland CO2 flux (Fang et al., 2018; Helbig et al., 2017; Zhang et al., 2016).

The daily carbon flux pattern is explained by the disappearance of photosynthesis at night during the growing season and, therefore, slower emissions at night and greater uptake during the day (Wang et al., 2022). At the end of the wetland vegetation growing season (September), the rate of CO2 emissions from the wetland peaked at dusk and dawn compared to other months. Conversely, at the beginning of the growing season (May), the carbon emission rates at dusk and dawn were slower than during the other months of the growing season. Carbon emissions from the wetland ecosystem exhibited an asymmetric emission pattern before and after the peak in NDVI during the growing season. That is, the high emissions of CO2 at dusk and dawn during the growing season were mainly concentrated at the end of the growing season. The reason for this phenomenon is likely that, at the beginning of the growing season, the primary productivity and ecological respiration rates of the wetland vegetation were relatively low, whereas, at the end of the growing season, productivity continuously declined and was accompanied by yellowing. Thus, the increase in the strength of respiration at the end of the growing season enhanced CO2 emissions. Mackelprang et al. also showed that freeze–thaw cycles accelerate the rate of soil respiration, leading to greenhouse gas emissions (Mackelprang et al., 2011). During the non-growing season, the wetland acted as a weak carbon sink approximately at midday (10:00 to 13:00) and a weak carbon source for the rest of the time. The low CO2 flux in the study area during the non-growing season in late winter—owing to the withering of vegetation, snow, and ice cover in late winter—and the high flux rate in spring resulted in weak photosynthesis and respiration rates in the wetland ecosystem. Numerous studies have corroborated the crucial role of snow and ice cover in the CO2 flux dynamics from cold wetlands, thereby inhibiting carbon emissions during winter (Aurela et al., 2001; Ohkubo et al., 2012).

https://doi.org/10.5194/egusphere-2024-2787
Preprint. Discussion started: 7 October 2024

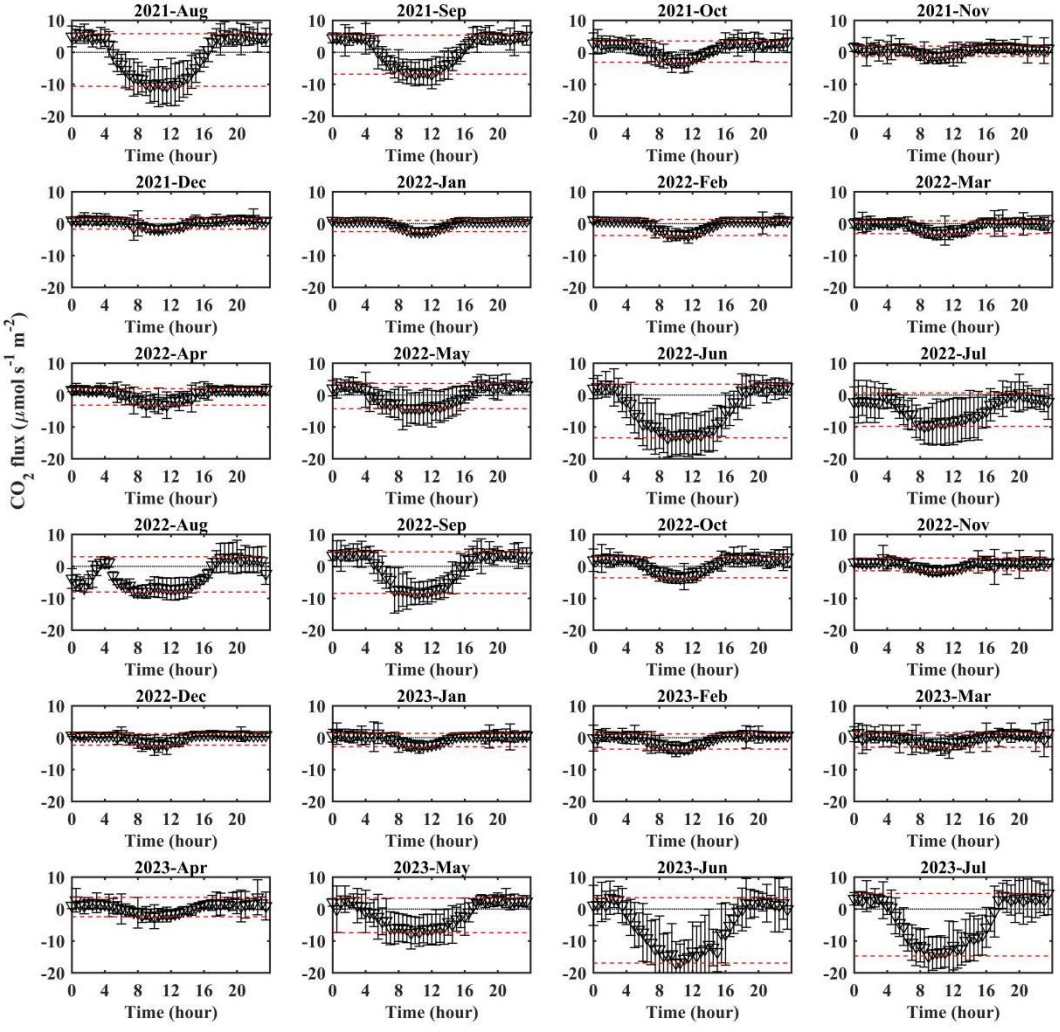

Figure 4: Monthly average variations in NEE from August 2021 to July 2023 over the Jingxin Wetland station.

3.3.2 Seasonal variations in CO_2 flux

Seasonal changes in the components of the CO2 balance are shown in Fig. 5. On a monthly scale, only weak CO2 emissions were observed in the wetlands in October 2021 and January 2022, and weak CO2 assimilation was observed in February–March 2022. In April, a transition from weak CO2 emission to higher CO2 emissions occurred; however, after April, during the growing season, CO2 flux became more notable in association with the initiation of spring growth and the increase in temperature, triggering respiration, melting of ice and snow, and increased soil carbon emissions. The CO2 flux was highest in June 2022 and June 2023, at 139.6 and 123.3 g C m-2 mon-1, respectively. The monthly average CO2 NEE during the growing season for the whole year of 2022 was –63.7 g C m-2 mon-1

https://doi.org/10.5194/egusphere-2024-2787
Preprint. Discussion started: 7 October 2024

compared to 4.56 g C m-2 mon-1 for the non-growing season. In comparison, the annual CO2 NEE in the same year was 353.6 g C m-2 yr-1, with an annual GPP of 763.83 g C m-2 yr-1 and a total annual Reco of 360.43C m-2 yr-1. These measurements indicate that the Jingxin Wetland has a higher net CO2 flux capacity when measured over an annual scale.

Interannual variations in net ecosystem CO2 exchange in wetlands can reflect the carbon source/sink efficacy of a particular ecosystem. The carbon balance in wetland ecosystems tends to vary owing to differences in vegetation cover and climatic conditions (Rankin et al., 2018). Among the cold wetlands located in the Qinghai-Tibetan Plateau region, the annual CO2 uptake observed in the alpine cold wetlands of Qinghai Lake was 246.7 g C m-2 yr-1 (Cao et al., 2017). Researchers have also found that the total annual CO2 assimilation in alpine peat wetlands on the northeastern Tibetan Plateau is 120.4 g C m-2 yr -1 (Zhu et al., 2020). In the cold-zone wetlands of the northeastern region, Wang studied CO2 dynamics in the peat bog wetlands in the Changbai Mountainous Region, and found that this area was a carbon sink in 2018 and 2019, with a cumulative uptake of 311.52 and 302.38 g C m-2 yr-1, respectively (Wang et al., 2022). Notably, we found similar results in our study area; thus, in general, the carbon sequestration capacity of the cold-zone wetlands in the northeastern region of China is higher than that of the cold-zone wetlands in the Qinghai-Tibet region (Table 1).

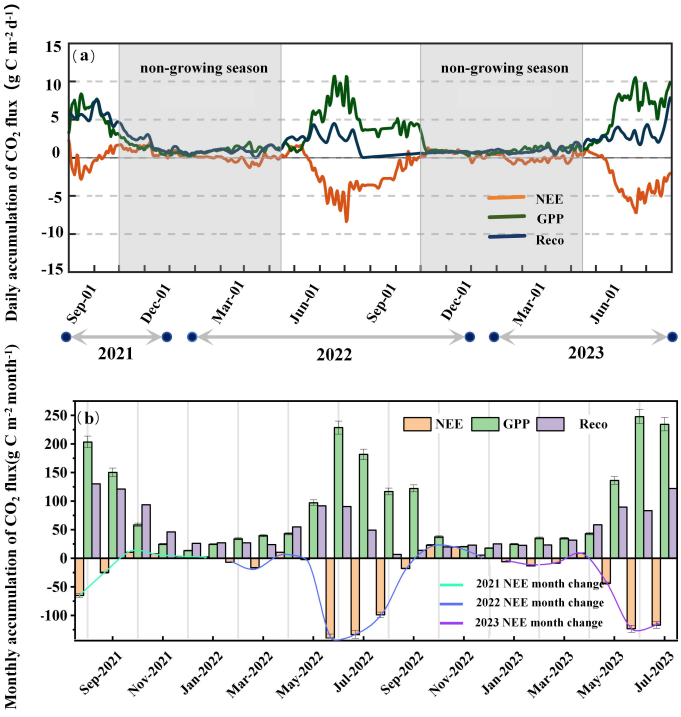

Figure 5: Cumulative carbon flux from August 2021 to July 2023 over the Jingxin Wetland station. (a). Daily totals. (b). Monthly total net ecosystem exchange, gross primary production (GPP), and ecosystem respiration (Reco).

https://doi.org/10.5194/egusphere-2024-2787
Preprint. Discussion started: 7 October 2024

Table 1 CO2 exchange capacity of wetlands in cold regions.

Site	Vegetation type	Determination time	NEE (g Cm^{-2} yr^{-1})	Longitude and latitude	References
Qinghai-Tibetan Plateau High cold wetland	moss	2005	86.18	37°37′N 101°19′E	(Fawei et al., 2008b)
Zoergai alpine wetland	meadow	2008–2009	–47.10 –79.70	33°56′N 102°52′E	(Hao et al., 2011a, b)
Alpine wetland meadow, Qinghai-Tibet Plateau	sedge	2004–2006	101.1 44.0 173.2	37°35′N 101°20′E	(Zhao et al., 2010)
Wetlands in the cold area of Ruoergai	moss	2013-2017	171.4±38.1	33°06′15.419″ N 102°39′05.278 ″E	(Liu et al., 2019)
Alpine wetland, Qinghai-Tibet Plateau	*Carex pamirensis*	2007–2016	120.4	37°35′N 101°209′E	(Zhu et al., 2020)
Alpine wetlands, Qinghai-Tibet Plateau	Marshy grassland	2015–2016	–211.85 to –53.84	37°44′N 100°05′E	(Cao et al., 2019)

https://doi.org/10.5194/egusphere-2024-2787
Preprint. Discussion started: 7 October 2024

3.4 Factors driving CO2 flux over different timescales in the Jingxin Wetland

3.4.1 Half-hourly fluxes

The relative importance of the main environmental factors affecting CO2 flux varied at different time scales in the Jingxin Wetland. At the half-hourly scale, NEE was mainly influenced by PPFD (Fig. 6), with the maximum photosynthetic rate during the growing season varying in the range 6.41–33.78 umol m-2 s-1, and the hourly NEE showed a rectangular hyperbolic relationship with PPFD (Fig. 7), as reported for many other types of wetland ecosystems (Du et al., 2021; Liu et al., 2009). During the growing season, the maximum NEE occurred in July 2022 (33.78 umol m-2 s-1) and June 2023 (31.39 umol m-2 s-1), and the maximum photosynthetic rate occurred in July, during the period of maximum vegetation growth (when the NDVI reached its maximum), which is in line with the results of a study on the photosynthetic rate of the reeds of the Songnen Plain (García-García et al., 2023). At the half-hourly scale, GPP is mainly influenced by PPFD, which is one of the main limiting factors (Ma et al., 2021; Zheng and Takeuchi, 2022).

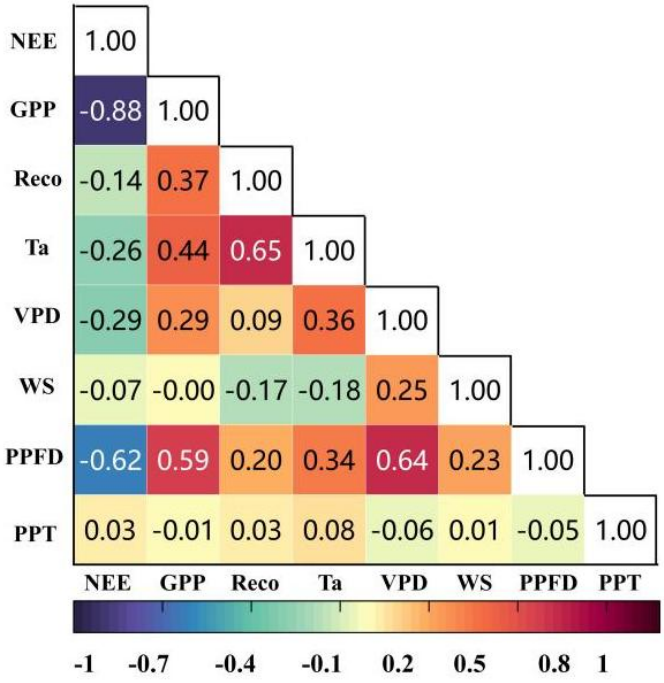

Figure 6: Relationships between Net Ecosystem Exchange (NEE) and meteorological factors on a half-hourly scale.

https://doi.org/10.5194/egusphere-2024-2787
Preprint. Discussion started: 7 October 2024

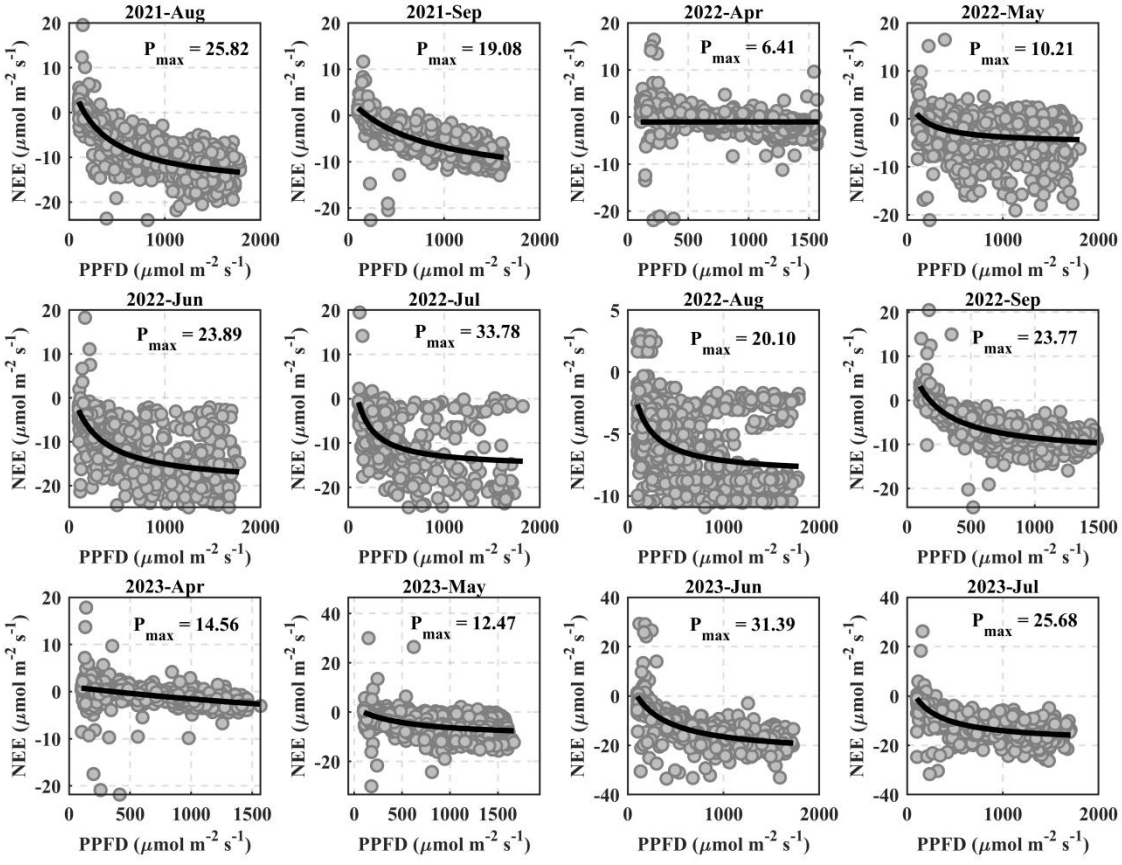

Figure 7: Maximum light energy utilization efficiency.

3.4.2 Daily fluxes

An aggregation analysis of NEE, GPP, and Reco for the environmental factors was performed using the partial least squares method (Fig. 8). The results show that Ta and VPD were the main environmental factors affecting carbon exchange, with an increase in VPD associated with an increase in the NEE value; that is, an increase in VPD limits the carbon-exchange capacity of wetland ecosystems. Note that the larger the NEE value, the weaker the carbon sequestration capacity of a wetland, and the smaller the value, the stronger is the carbon sequestration capacity. Multiple stepwise regression analyses of NEE, GPP, and Reco with the potential environmental factors of PPFD, Ta, PPT, VPD, and Wind Speed (WS) showed that Ta, PPFD, and VPD were the main factors affecting the overall change in NEE during the growing season (Table 2), whereas only Reco was significantly affected by Ta during the non-growing season. Temperature plays an important role in many environmental processes that affect CO2 fluxes

https://doi.org/10.5194/egusphere-2024-2787
Preprint. Discussion started: 7 October 2024

(Jauhiainen et al., 2012). Notably, Reco is affected more by temperature than GPP, mainly because respiration is more dependent on temperature than photosynthesis, and Reco increases exponentially with temperature (Lloyd and Taylor, 1994; Nakano et al., 2022). VPD is an important environmental factor affecting the photosynthetic capacity of ecosystems. This indicates that the dryness of air reflects the comprehensive influence of temperature and humidity and controls the physiological processes of plant photosynthesis by affecting stomatal closure (Turner et al., 1984). Previous studies have shown that PPFD is a key factor affecting CO2 flux, which, in turn, affects plant photosynthesis and controls temperature. High radiation is beneficial for photosynthesis and respiration and directly affects the carbon sink intensity of wetland ecosystems in cold regions (Cao et al., 2017). In this study, PPFD was considered to be one of the important factors regulating the diurnal and seasonal variations in CO2 fluxes contributing to GPP and NEE; however, VPD was more sensitive to diurnal and seasonal variations, indicating that the effects of temperature and humidity—as reflected by VPD—and the associated changes in plant physiology best reflect the changes in CO2 in the study area.

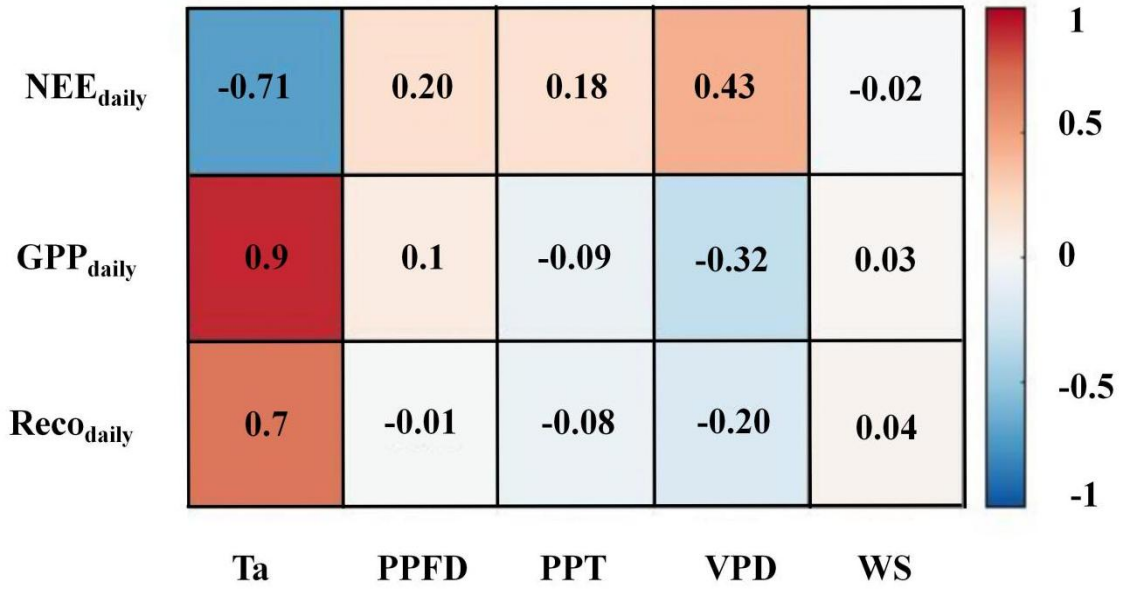

Figure 8: Correlations between daily carbon exchange and meteorological factors.

https://doi.org/10.5194/egusphere-2024-2787
Preprint. Discussion started: 7 October 2024

Table 2 Multiple stepwise regression of CO2 exchange rate and environmental factors (S1/S2). Note that as rainfall (PPT) in the growing season/non-growing season was not significant in the multiple regression, these values are not shown.

Stepwise regression equation	R^2	P	Ta	PPFD	PPT	VPD	WS
NEE (S1) = –0.11Ta + 0.29VPD –0.005PPFD + 0.484WS	0.56	< 0.01	–0.33	–0.49	-	0.54	-
NEE (S2) = 0.045Ta – 0.022VPD + 0.076WS	0.30	< 0.01	0.90	-	-	–0.31	0.18
GPP (S1) = 0.21Ta –0.32VPD + 0.007PPFD	0.86	< 0.01	0.54	0.51	-	–0.48	-
Reco (S1) = 0.08Ta 0.17VPD + 0.005PPFD	0.70	< 0.01	0.47	0.23	-	–0.26	-
Reco (S2) = 0.09Ta + 0.3VPD	0.54	< 0.01	0.80	-	-	–0.40	-

3.5 Energy budget changes and controls

3.5.1 Changes in energy budget components

The composition of the heat flux is shown in Fig. 9. The heat distribution was mainly high during the growing season and low during the non-growing season. Latent heat energy accounted for 73.5% of the radiant energy throughout the year, indicating that the study area is mainly controlled by LE energy. The distribution of latent heat energy accounted for 90.3% of the solar radiation energy in the growing season, indicating that the distribution of latent heat energy dominates the energy distribution during the growing season; thus, the variation in latent heat energy in the growing season has a major impact on climate change in the study area. The seasonal variation in net radiation was stronger, and the average value was larger than that in the non-growing season. The maximum Rn occurred in July 2022, at 294.5 W m-2, and the seasonal variation in LE was similar with a maximum daily average also occurring in July 2022, at 209.9 W m-2. This is similar to the artificial semi-arid reed wetlands in Zhangye, China (Zhang et al., 2016). However, 60% of the Rn in the alpine riparian ecosystems on the Tibetan Plateau is consumed by H rather than LE (Zhang et al., 2014). The difference in energy flux between the growing and non-growing seasons may be mainly caused by vegetation, which plays an important role in regulating radiation absorption and energy distribution through leaf reflection, photosynthesis, and transpiration (Sun et al., 2017). Thus, the presence of vegetation changes the energy allocation and increases the proportion in the growing season through transpiration (Dare-Idowu et al., 2021).

https://doi.org/10.5194/egusphere-2024-2787
Preprint. Discussion started: 7 October 2024

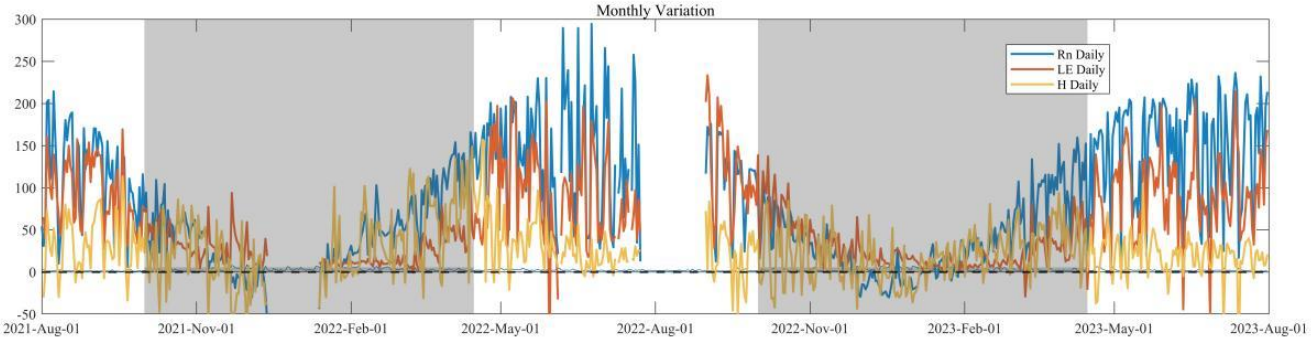

330 **Figure 9: Changes in the energy budget. Daily average net radiation (Rn, W m-2), sensible heat flux (H, W m-2), and latent heat flux (LE, W m-2) from August 2021 to July 2023 over the Jingxin Wetland station.**

3.5.2 Controls of H and LE

LE is mainly controlled by half-hourly and diurnal Rn, and LE and meteorological variables are more closely
335 associated during the growing season than during the non-growing season (Fig. 10). Generally, LE had a greater influence on environmental factors during the growing season than during the non-growing season, and the influence of H on environmental factors was not affected by season. LE had a greater influence on VPD in the Jingxin Wetland at half-hourly and daily scales (Fig. S2). On a daily scale, LE showed a significant positive correlation with VPD during the growing season (Table 3). During the non-growing season, LE has a weak effect on all environmental
340 factors and H becomes the main heat-affecting regional climatic factor during the non-growing season, affecting variations in Ta during the non-growing season (García-García et al., 2023). The latent heat flux of the reed wetlands remained positive throughout the study period, reflecting their strong water-cycling characteristics; water vapor was consistently transported upward throughout the day. In contrast, in the Qinghai-Tibet Plateau region, the latent heat flux tends to be relatively weak and VPD also shows less fluctuation (Fawei et al., 2008a). Therefore, LE affects
345 atmospheric VPD and Ta via the water phase-change process and, ultimately, affects CO2 fluxes in the Jingxin Wetland.

https://doi.org/10.5194/egusphere-2024-2787
Preprint. Discussion started: 7 October 2024

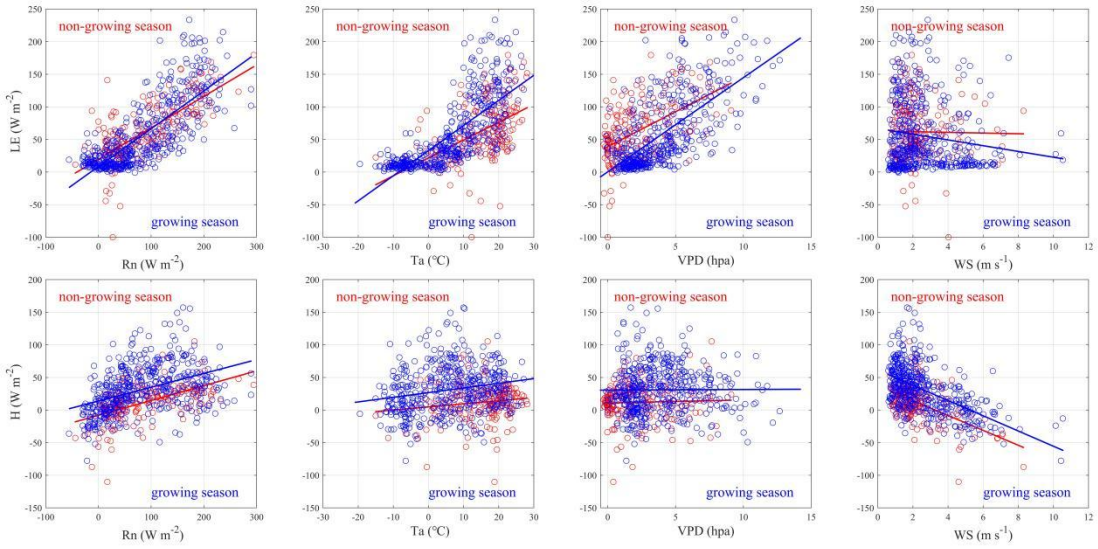

Figure 10: Relationships between latent heat flux (LE) and net radiation (Rn), air temperature (Ta), vapor pressure deficit (VPD), and wind speed (WS); and between half-hourly sensible heat flux (H) and Rn, Ta, VPD, and WS for the growing and non-growing seasons between August 2021 and July 2023 over the Jingxin Wetland station.

Table 3 Latent heat, sensible heat, and the sensitivity of meteorological factors. On a daily scale, environmental factors are partially correlated with LE (relationships between sensible heat flux (H), latent heat flux (LE), and meteorological variables including net radiation (Rn), air temperature (Ta), vapor pressure deficit (VPD), and wind speed (WS) between August 2021 and July 2023 were considered. ** and * indicate p = 0.01 and p = 0.05, respectively.

Season		Rn	Ta	VPD	WS
Overall	H	0.91**	0.80**	0.23**	–0.61**
	LE	0.45**	0.35**	0.53**	0.15
Growing	H	0.59**	0.06	0.44	0.19
	LE	0.43**	0.33**	0.45**	0.12
Non-growing	H	0.3**	0.4**	0.003	–0.52**
	LE	0.20**	0.37**	0.26**	0.38

https://doi.org/10.5194/egusphere-2024-2787
Preprint. Discussion started: 7 October 2024

4 Conclusions

We examined fluctuations in carbon dioxide exchange in the Jingxin Wetland over various temporal scales and explored the interconnection between climatic drivers, energy budgets, and CO2 flux. The Jingxin Wetland exhibits strong carbon sequestration capabilities, with a total annual average carbon dioxide absorption during the research period of 362.3 g C m-2 yr-1. On a half-hourly scale, NEE was predominantly controlled by the PPFD, while on a daily scale, VPD emerged as the primary driver of carbon exchange. During the growing season, VPD constrained GPP, thus becoming the main environmental factor influencing NEE. In contrast, Ta played a primary role in controlling Reco during the non-growing season. During the growing season, LE significantly affected VPD, indicating that the regulation of carbon dioxide flux by VPD in the Jingxin Wetland was mainly affected by LE.

Data availability

All data are available in the main text or supplementary material. All the code used in this study will be provided by the corresponding author upon reasonable request.

Author contributions

Jihao Zhang: Conceptualization, methodology, formal analysis, investigation, data curation, visualization, and writing—original draft preparation. Pengshen Chen: Conceptualization, methodology, formal analysis, investigation, data curation, visualization, and writing—original draft preparation. Duqi Liu: Investigation, methodology, formal analysis, investigation, data curation, visualization, and writing — original draft preparation. Ruihan Liang: Investigation, methodology, formal analysis, investigation, data curation, visualization, and writing—original draft preparation. Guishan Cui: Investigation, writing, reviewing, editing, supervision, project administration, and funding acquisition.

Competing interests

All authors declare that they have no conflicts of interest.

https://doi.org/10.5194/egusphere-2024-2787
Preprint. Discussion started: 7 October 2024

Financial support

This study was supported by the National Natural Science Foundation of China (grant numbers 42276177) and the Natural Science Foundation of Jilin Province (grant number YDZJ202401395ZYTS).

References

Aurela, M., Laurila, T., and Tuovinen, J. P.: Seasonal CO2 balances of a subarctic mire, Journal of Geophysical Research: Atmospheres, 106, 1623-1637, https://doi.org/10.1029/2000JD900481, 2001.

Cao, S., Cao, G., Chen, K., Han, G., Liu, Y., Yang, Y., and Li, X.: Characteristics of CO2, water vapor, and energy exchanges at a headwater wetland ecosystem of the Qinghai Lake, Canadian Journal of Soil Science, 99, 227-243, https://doi.org/10.1139/cjss-2018-0104, 2019.

Cao, S., Cao, G., Feng, Q., Han, G., Lin, Y., Yuan, J., Wu, F., and Cheng, S.: Alpine wetland ecosystem carbon sink and its controls at the Qinghai Lake, Environmental Earth Sciences, 76, 1-15, https://doi.org/10.1007/s12665-017-6529-5, 2017.

Chapin, F. S., Matson, P. A., Mooney, H. A., and Vitousek, P. M.: Principles of terrestrial ecosystem ecology, https://doi.org/10.1007/978-1-4419-9504-9, 2002.

Coffer, M. M. and Hestir, E. L.: Variability in trends and indicators of CO2 exchange across arctic wetlands, Journal of Geophysical Research: Biogeosciences, 124, 1248-1264, https://doi.org/10.1029/2018JG004775, 2019.

Dare-Idowu, O., Brut, A., Cuxart, J., Tallec, T., Rivalland, V., Zawilski, B., Ceschia, E., and Jarlan, L.: Surface energy balance and flux partitioning of annual crops in southwestern France, Agricultural and Forest Meteorology, 308, 108529, https://doi.org/10.1016/j.agrformet.2021.108529, 2021.

Du, Q., Liu, H., Liu, Y., Xu, L., and Sun, J.: Water and carbon dioxide fluxes over a “floating blanket” wetland in southwest of China with eddy covariance method, Agricultural and Forest Meteorology, 311, 108689, https://doi.org/10.1016/j.agrformet.2021.108689, 2021.

Fang, Q., Wang, G., Liu, T., Xue, B.-L., and Yinglan, A.: Controls of carbon flux in a semi-arid grassland ecosystem experiencing wetland loss: vegetation patterns and environmental variables, Agricultural and Forest Meteorology, 259, 196-210, https://doi.org/10.1016/j.agrformet.2018.05.002, 2018.

Fawei, Z., Hongqin, L., Yingnian, L., and Liang, Z.: Surface energy partitioning in alpine swamp meadow in the Qinghai Tibetan Plateau, 2008a.

Fawei, Z., Anhua, L., Yingnian, L., Liang, Z., Qinxue, W., and Mingyuan, D.: CO2 flux in alpine wetland ecosystem on the Qinghai-Tibetan Plateau, China, Acta Ecologica Sinica, 28, 453-462, https://doi.org/10.1016/S1872-2032(08)60024-4, 2008b.

https://doi.org/10.5194/egusphere-2024-2787
Preprint. Discussion started: 7 October 2024

García-García, A., Cuesta-Valero, F. J., Miralles, D. G., Mahecha, M. D., Quaas, J., Reichstein, M., Zscheischler, J., and Peng, J.: Soil heat extremes can outpace air temperature extremes, Nature Climate Change, 13, 1237-1241, https://doi.org/10.1038/s41558-023-01812-3, 2023.

Han, L., Mu, C., Jiang, N., Shen, Z., Chang, Y., Hao, L., and Peng, W.: Responses of seven wetlands carbon sources and sinks to permafrost degradation in Northeast China, Journal of Soils and Sediments, 23, 15-31, https://doi.org/10.1007/s11368-022-03271-3, 2023.

Hao, Y. B., Cui, X. Y., Wang, Y. F., Mei, X. R., Kang, X. M., Wu, N., Luo, P., and Zhu, D.: Predominance of Precipitation and Temperature Controls on Ecosystem CO2 Exchange in Zoige Alpine Wetlands of Southwest China, Wetlands, 31, 413-422, https://doi.org/10.1007/s13157-011-0151-1, 2011a.

Hao, Y. B., Cui, X. Y., Wang, Y. F., Mei, X. R., Kang, X. M., Wu, N., Luo, P., and Zhu, D.: Predominance of precipitation and temperature controls on ecosystem CO 2 exchange in Zoige alpine wetlands of Southwest China, Wetlands, 31, 413-422, https://doi.org/10.1007/s13157-011-0151-1, 2011b.

Helbig, M., Chasmer, L. E., Desai, A. R., Kljun, N., Quinton, W. L., and Sonnentag, O.: Direct and indirect climate change effects on carbon dioxide fluxes in a thawing boreal forest–wetland landscape, Global Change Biology, 23, 3231-3248, https://doi.org/10.1111/gcb.13638, 2017.

Jauhiainen, J., Hooijer, A., and Page, S.: Carbon dioxide emissions from an Acacia plantation on peatland in Sumatra, Indonesia, Biogeosciences, 9, 617-630, https://doi.org/10.5194/bg-9-617-2012, 2012.

Liu, X., Zhu, D., Zhan, W., Chen, H., Zhu, Q., Hao, Y., Liu, W., and He, Y.: Five-year measurements of net ecosystem CO2 exchange at a fen in the Zoige peatlands on the Qinghai-Tibetan Plateau, Journal of Geophysical Research: Atmospheres, 124, 11803-11818, https://doi.org/10.1029/2019JD031429, 2019.

Liu, Z., Zhu, W., Nan, Y., Seng, B., Wang, Q., and Zhao, Y.: Change of Jingxin Wetland in the lower reaches of Tumen River based on Corona and SPOT-5 images, Wetl. Sci, 7, 237-242, 2009.

Lloyd, J. and Taylor, J.: On the temperature dependence of soil respiration, Functional ecology, 315-323, https://doi.org/10.2307/2389824, 1994.

Ma, Y., Yue, X., Zhou, H., Gong, C., Lei, Y., Tian, C., and Cao, Y.: Identifying the dominant climate-driven uncertainties in modeling gross primary productivity, Science of The Total Environment, 800, 149518, https://doi.org/10.1016/j.scitotenv.2021.149518, 2021.

Mackelprang, R., Waldrop, M. P., DeAngelis, K. M., David, M. M., Chavarria, K. L., Blazewicz, S. J., Rubin, E. M., and Jansson, J. K.: Metagenomic analysis of a permafrost microbial community reveals a rapid response to thaw, Nature, 480, 368-371, https://doi.org/10.1038/nature10576, 2011.

Nakano, D., Iwata, T., Suzuki, J., Okada, T., Yamamoto, R., and Imamura, M.: The effects of temperature and light on ecosystem metabolism in a Japanese stream, Freshwater Science, 41, 113-124, https://doi.org/10.1086/718648, 2022.

https://doi.org/10.5194/egusphere-2024-2787
Preprint. Discussion started: 7 October 2024

Neubauer, S. C. and Verhoeven, J. T.: Wetland effects on global climate: mechanisms, impacts, and management recommendations, Wetlands: ecosystem services, restoration and wise use, 39-62, https://doi.org/10.1007/978-3-030-14861-4_3, 2019.

Ohkubo, S., Iwata, Y., and Hirota, T.: Influence of snow-cover and soil-frost variations on continuously monitored CO2 flux from agricultural land, Agricultural and forest meteorology, 165, 25-34, https://doi.org/10.1016/j.agrformet.2012.06.012, 2012.

Rankin, T., Strachan, I., and Strack, M.: Carbon dioxide and methane exchange at a post-extraction, unrestored peatland, Ecological Engineering, 122, 241-251, https://doi.org/10.1016/j.ecoleng.2018.06.021, 2018.

Schuur, E. A., Bockheim, J., Canadell, J. G., Euskirchen, E., Field, C. B., Goryachkin, S. V., Hagemann, S., Kuhry, P., Lafleur, P. M., and Lee, H.: Vulnerability of permafrost carbon to climate change: Implications for the global carbon cycle, BioScience, 58, 701-714, https://doi.org/10.1641/B580807, 2008.

Shen, X., Liu, B., Xue, Z., Jiang, M., Lu, X., and Zhang, Q.: Spatiotemporal variation in vegetation spring phenology and its response to climate change in freshwater marshes of Northeast China, Science of The Total Environment, 666, 1169-1177, https://doi.org/10.1016/j.scitotenv.2019.02.265, 2019.

Sun, X., Zou, C., Wilcox, B. P., and Stebler, E.: Effect of vegetation on the energy balance and evapotranspiration in tallgrass prairie: a paired study with eddy covariance systems, AGU Fall Meeting Abstracts, B51G-1900, https://doi.org/10.1007/s10546-018-0388-9,

Tan, Y., Wang, X., Yang, Z., and Wang, Y.: Research progress in cold region wetlands, China, Sciences in Cold and Arid Regions, 3, 441-447, https://doi.org/10.3724/SP.J.1226.2011.00441, 2011.

Turner, N. C., Schulze, E.-D., and Gollan, T.: The responses of stomata and leaf gas exchange to vapour pressure deficits and soil water content: I. Species comparisons at high soil water contents, Oecologia, 63, 338-342, https://doi.org/10.1007/BF00390662, 1984.

Vickers, D. and Mahrt, L.: Quality control and flux sampling problems for tower and aircraft data, Journal of atmospheric and oceanic technology, 14, 512-526, https://doi.org/10.1175/1520-0426(1997)014<0512:QCAFSP>2.0.CO;2, 1997.

Wang, B., Mu, C., Lu, H., Li, N., Zhang, Y., and Ma, L.: Ecosystem carbon storage and sink/source of temperate forested wetlands in Xiaoxing'anling, northeast China, Journal of Forestry Research, 33, 839-849, https://doi.org/10.1007/s11676-021-01366-0, 2022.

WANG, D.-X., GAO, Y.-H., AN, X.-J., WANG, R., and XIE, Q.-Y.: Responses of greenhouse gas emissions to water table fluctuations in an alpine wetland on the Qinghai-Tibetan Plateau, Acta Prataculturae Sinica, 25, 27, https://doi.org/10.11686/cyxb2016012, 2016.

Webb, E. K., Pearman, G. I., and Leuning, R.: Correction of flux measurements for density effects due to heat and water vapour transfer, Quarterly Journal of the Royal Meteorological Society, 106, 85-100, https://doi.org/10.1002/qj.49710644707, 1980.

https://doi.org/10.5194/egusphere-2024-2787
Preprint. Discussion started: 7 October 2024

Wei, D. and Wang, X.: Uncertainty and dynamics of natural wetland CH4 release in China: Research status and priorities, Atmospheric Environment, 154, 95-105, https://doi.org/10.1016/j.atmosenv.2017.01.038, 2017.

Wei, D., Zhao, H., Huang, L., Qi, Y., and Wang, X.: Feedbacks of alpine wetlands on the Tibetan Plateau to the atmosphere, Wetlands, 40, 787-797, https://doi.org/10.1007/s13157-019-01220-4, 2020.

Wilczak, J. M., Oncley, S. P., and Stage, S. A.: Sonic anemometer tilt correction algorithms, Boundary-layer meteorology, 99, 127-150, https://doi.org/10.1023/A:1018966204465, 2001.

Zhang, Q., Sun, R., Jiang, G., Xu, Z., and Liu, S.: Carbon and energy flux from a Phragmites australis wetland in Zhangye oasis-desert area, China, Agricultural and Forest Meteorology, 230, 45-57, https://doi.org/10.1016/j.agrformet.2016.02.019, 2016.

Zhang, S.-Y., Li, X.-Y., Ma, Y.-J., Zhao, G.-Q., Li, L., Chen, J., Jiang, Z.-Y., and Huang, Y.-M.: Interannual and seasonal variability in evapotranspiration and energy partitioning over the alpine riparian shrub Myricaria squamosa Desv. on Qinghai–Tibet Plateau, Cold Regions Science and Technology, 102, 8-20, https://doi.org/10.1016/j.coldregions.2014.02.001, 2014.

Zhao, L., Li, J., Xu, S., Zhou, H., Li, Y., Gu, S., and Zhao, X.: Seasonal variations in carbon dioxide exchange in an alpine wetland meadow on the Qinghai-Tibetan Plateau, Biogeosciences, 7, 1207-1221, https://doi.org/10.5194/bg-7-1207-2010, 2010.

Zhao, M., Liu, Y., and Zhang, X.: A review of research advances on carbon sinks in farmland ecosystems, Acta Ecol. Sin, 42, 9405-9416, https://doi.org/10.5846/stxb202203280762, 2022.

Zheng, Y. and Takeuchi, W.: Estimating mangrove forest gross primary production by quantifying environmental stressors in the coastal area, Scientific Reports, 12, 2238, https://doi.org/10.1038/s41598-022-06231-6, 2022.

Zhu, J., Zhang, F., Li, H., He, H., Li, Y., Yang, Y., Zhang, G., Wang, C., and Luo, F.: Seasonal and interannual variations of CO2 fluxes over 10 years in an alpine wetland on the Qinghai-Tibetan Plateau, Journal of Geophysical Research: Biogeosciences, 125, e2020JG006011, https://doi.org/10.1029/2020JG006011, 2020.